https://doi.org/10.20965/jaciii.2016.p0155



**Paper:**

# Research on Cross-Correlative Blur Length Estimation Algorithm in Motion Blur Image

**Li Dongming**[*1], **Su Zhengbo**[*2], **Su Wei**[*3,†], **and Zhang Lijuan**[*4]

[*1]School of Information Technology, Jilin Agriculture University
No.2888, XinCheng Street, Changchun City, Jilin 130118, China
E-mail: ldm0214@163.com
[*2]School of Computer Science and Technology, Harbin Institute of Technology
92 West Dazhi Street, Harbin, Heilongjiang 150001, China
E-mail: szbbob@126.com
[*3]Informatization Center, Changchun University of Science and Technology
No.7089, Rd. Weixing, Changchun, Jilin 130022, China
E-mail: sw@cust.edu.cn
[*4]College of Computer Science and Engineering, Changchun University of Technology
No.2055, YanAn Street, Changchun City, Jilin 130012, China
[†]Corresponding author

[Received November 10, 2015; accepted December 10, 2015]

**This paper proposes a motion blur length estimation method that is applied to motion blur image restoration. This method applies a cross-correlation algorithm to multi-frame motion-degraded images. In order to find the motion blur parameters, the Radon transform method is used to estimate the motion blur angle. We extract the gray value of pixels around the blur center, calculate the correlation for obtaining motion blur length, and use the Lucy-Richardson iterative algorithm to restore the degraded image. Experiment results show that this method can accurately estimate blur parameters, reduce noise, and obtain better restoration results. The method achieves good results on artificially blurred images and natural images (by the camera shake). The advantage of our algorithm that uses the Lucy-Richardson restoration algorithm compared with the Wiener filtering algorithm is made obvious with less computation time and better restored effects.**

**Keywords:** cross correlation, motion blur image, blur length, point spread function (PSF), radon transform

## 1. Introduction

There are many reasons for motion blur in photographic images, such as the impact of atmospheric turbulence, and camera movement or shake. The blurry image caused by relative motion between the camera and scene is called the motion blur image [1]. A restoration algorithm for motion blur images is currently one of the popular studies, and has attracted the attention of domestic and international scholars. Such algorithm has been widely used in the fields of medical imaging, road traffic detection, military detection, etc.

In recent years, many researchers have presented algorithms to estimate motion blur parameters. Chan [2] proposed total variation (TV) regularization. Certain regularization terms have to be added in the minimization, and thus Chan's method is suitable for out-of-focus blurring on medical or satellite images. In the case of motion blurring, TV regularization is not a good choice. Mayntz [3] studied blur identification using a spectral inertia tensor and spectral zeros. His method requires a prior parametric knowledge of the PSF. Chang [4] proposed blur identification method by using bispectrum, thus finding motion blur parameters when there is no additive noise. The author attempted to model bispectrum by adopting the Auto-Regressive Moving Average (ARMA) model, and he employed this method for finding PSF coefficients. Therefore, the aforementioned algorithms are completely different from the algorithm presented in this paper.

In this paper, a new motion blur length estimation algorithm based on the correlation principle is proposed. First, we obtain the estimates of the blurred motion angle according to the Radon transform results. Second, we select the center of the blur and set the radius according to the blur angle extracted by the pixel gray value of each blur path on the blur center, and then perform a cross-correlation calculation with the candidate PSF in order to find the maximum point of the cross-correlation, i.e., the blur length. Finally, we restore the observed image using the Lucy-Richardson iterative algorithm.

## 2. Degradation Model and Blur Parameter Estimation

The motion blur image are those that have noise whose restoration relies largely on PSF estimates. A blur image

is theoretically modeled by a convolution in the space domain, as follows:

$$g = f \otimes h + n \quad \ldots\ldots\ldots\ldots\ldots\ldots \quad (1)$$

where $g$ is the observed blurred image, $f$ is the ideal image (i.e., if the camera would not move), $\otimes$ represents the convolution operation, $h$ is PSF, and $n$ is noise (usually caused by a camera sensor).

Typically, image processing in the frequency domain is faster than in the space domain. The corresponding model can be described as follows:

$$G = F \cdot H + N \quad \ldots\ldots\ldots\ldots\ldots\ldots \quad (2)$$

Let the capital letters denote the two-dimensional Discrete Fourier Transforms of the respective lower case letters, and $\cdot$ represent the element-wise multiplication. In Fourier analysis of the optical system, the degradation function $H$ is sometimes called the Optical Transfer Function (OTF) [5]. In the space domain, $h$ is PSF. In the aerodynamic flow field, the OTF can be obtained by the Fourier transform of PSF, as follows:

$$H(u,v) = \int_{-\infty}^{\infty}\int_{-\infty}^{\infty} h(x,y)\exp[-j2\pi(ux+vy)]dxdy \quad (3)$$

where $(x,y)$ is the two-dimensional coordinates in the space domain, $(u,v)$ is the two-dimensional coordinates in the frequency domain, and $H(u,v)$ is the Fourier transform of PSF $h(x,y)$.

From Eq. (3), we know that the main task of motion blur image restoration is to estimate PSF.

### 2.1. Motion Blur Properties

The mathematical model for the PSF of motion blur images is as follows [6]:

$$h(x,y) = \begin{cases} \dfrac{1}{a} & \text{if } \sqrt{x^2+y^2} \le \dfrac{a}{2} \text{ and } \dfrac{x}{y} = -\tan(\phi) \\ 0 & \text{others} \end{cases} \quad (4)$$

From Eq. (4) we can see that PSF depends on two parameters: moving direction ($\phi$) and length ($a$). **Fig. 1** shows the noise-free motion blur and spectrogram of a Lena image.

**Figure 1** shows that the spectrogram of the noise-free observation image of motion blur displays many parallel black lines. In order to further study the movement of the noisy blurred image, we artificially add Gaussian noise to the image shown in **Fig. 1(a)** with a blur length of 20 pixels, angle of 45°, and density noise of 0.02 in order to experiment with the $256 \times 256$ Lena image; this results in the noisy blurred image and spectrogram shown in **Figs. 1(c)** and **1(d)**. **Fig. 1(c)** is the $256 \times 256$ linear noisy blurred image with blur parameter $L = 20$ pixels and $\phi = 45°$ with Gaussian noise density of 0.02. **Fig. 1(d)** is the spectrogram of **Fig. 1(c)**.

**Figure 1(d)** shows that after adding noise to the motion blur image, the parallel black lines become weak or even disappear from the spectrogram. If the variation of noise

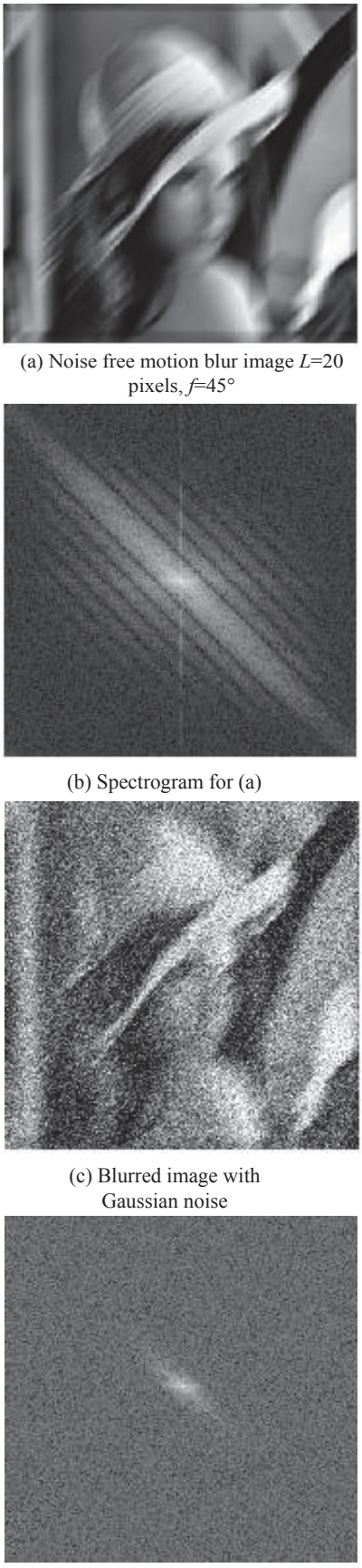

(a) Noise free motion blur image $L$=20 pixels, $f$=45°

(b) Spectrogram for (a)

(c) Blurred image with Gaussian noise

(d) Spectrogram for (c)

**Fig. 1.** Motion blur and spectrogram of Lena image.

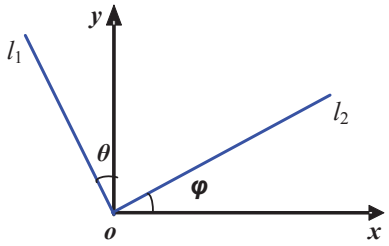


**Fig. 2.** Relationship of parallel black lines between motion blur direction and Fourier spectrum.

were to increase, many parallel black lines might disappear. In order to estimate the motion blur parameters of the image with noise, we use the noisy image as the input, as proposed in [7]. By using the noise removal method on the observation image $g(x,y)$ for image processing, and then employing the denoised images $g'(x,y)$ as the input for estimating the degraded image, the important information necessary for estimating blur parameters [8] is simultaneously removed.

## 2.2. Blur Angle Estimation

The motion blur direction $\varphi$ is equivalent to angle $\theta$, as shown in **Fig. 2**, where line $l_1$ is a spectrum parallel black line in the figure, line $l_1$ and line $l_2$ are vertical, angle $\theta$ is the angle included between line $l_1$ and the $y$-axis, and angle $\varphi$ is the angle included between line $l_2$ and the $x$-axis. Then, it can be concluded that $\varphi = \theta$ by the triangle theorem.

The methods for estimating the directions of noise-free and noisy blur motion are the same. We use the logarithmic of the Fourier transform and perform Radon transform. In the Radon domain, the peak appears on the corresponding angle. Therefore, the motion angle can be obtained.

The Radon transform [8] is used to calculate the projection of the image matrix in a certain direction. For binary images, if the integral is large in a certain direction, it is strongly linear in that direction, i.e., this indicates the existence of segments. Unlike the Hough transform [9], the Radon transform can show the lines in an image without specific points in the coordinates [9]. In order to detect the linear direction, we define:

$$I(x,y) = \log_2(|G(u,v)|) \quad \ldots\ldots\ldots\ldots (5)$$

where $(x,y)$ is the two-dimensional coordinates in the space domain, $(u,v)$ is the two-dimensional coordinates in the frequency domain, and $G(u,v)$ is the Fourier transform of the observed image $g(x,y)$. $I(x,y)$ is the grayscale image of the space domain. We then perform Radon transform on Eq. (5) to obtain:

$$R(\rho,\theta) = \int_{-\infty}^{+\infty}\int_{-\infty}^{+\infty} I(x,y)\delta(\rho - x\cos\theta - y\sin\theta)dxdy \quad \ldots (6)$$

The motion angle estimation of the blurred image is shown in **Fig. 3**, which demonstrates the Radon transform

(a) Edge of motion blur image

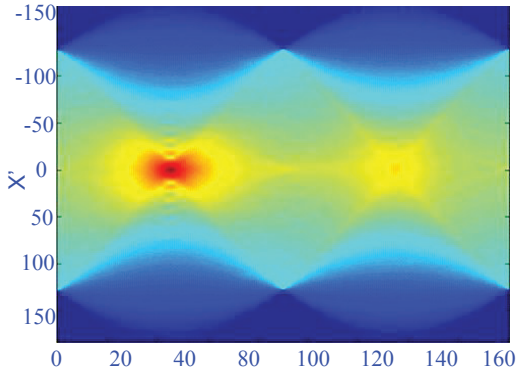


(b) Radon transform of Fourier spectrum

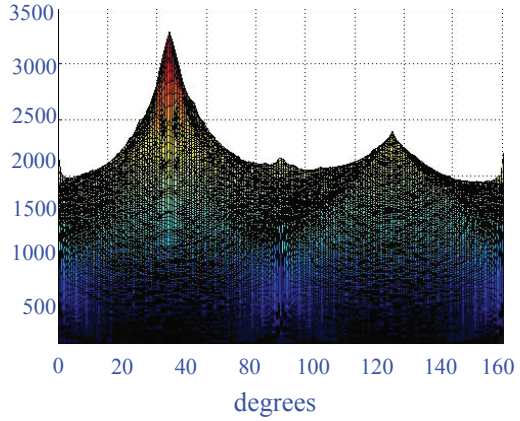


(c) Result of Radon transform

**Fig. 3.** Motion angle estimation of blurred image.

of image **Fig. 1(a)**. **Fig. 3(a)** is the edge of the motion blurred image shown in **Fig. 1(a)**, **Fig. 3(b)** is the Radon transform of the Fourier spectrum, and **Fig. 3(c)** is the result of the Radon transform.

We use the improved Radon transform to estimate the motion blur angle, and the algorithm is summarized as follows:

*i. In order to highlight the trajectory of the motion blurred image, first detect the blurred image edge; the edge detection operator should be isotropic, and thus the Gauss-Laplace filter is used. That is, observe image g as the input image, and then detect the image edge to obtain image BW.*

*ii. F is the fast Fourier transform of image BW that is the BW transform of the frequency domain, and obtains the spectrum map.*

*iii. $I = \log(1 + \mathrm{abs}(F))$ can be obtained based on exponential F, and then the Radon transform is performed.*

*iv. Based on the result of the transform, detect the maximum projection position in the x direction, namely, the estimation of the motion blur angle.*

### 2.3. Blur Length Estimation

In motion blurred images, blur length refers to the width of the blur band formed by the target points in the observed image. In this paper, we use the cross-correlation method proposed by Bonmassar and Schwartz [10], whose computation complexity is low.

The following Eq. (7) is used to calculate the correlation between $g$ and $\hat{h}$ [11]. Where $g = [g(0)g(1)\ldots g(N-1)]^T$ is grayscale in the blur direction, $\hat{h}$ is the Fourier spectrum of PSF candidate sets.

$$Corr(g,\hat{h}) = \log_2(|G|) \circ \log_2(|\hat{H}(\hat{a})|) = \frac{\sum_n [\log_2(\varepsilon + |G(u)| - \mu_G)]\left[\log_2(\varepsilon + |\hat{H}(u)| - \mu_{\hat{H}})\right]}{\left\{\sum_n [\log_2(\varepsilon + |G(u)| - \mu_G)]^2\right\}^{\frac{1}{2}} \cdot \left\{\sum_n \left[\log_2(\varepsilon + |\hat{H}(u)| - \mu_{\hat{H}}\right]^2\right\}^{\frac{1}{2}}} \quad \ldots\ldots (7)$$

where $G$ is the discrete Fourier transform of $g$; $\hat{H}$ is the discrete Fourier transform of the candidate PSF $\hat{h}$ (associated with the blur length of the candidate); $\varepsilon$ is a small positive constant used to avoid logarithmic equaling to zero; $\circ$ refers to the cross-correlation operation; and $\mu_G$ and $\mu_{\hat{H}}$ are the mean value of $|G|$ and $|\hat{H}|$, respectively:

$$\mu_G = \frac{1}{n}\sum_{u=1}^{n} G(u) \quad \ldots\ldots (8)$$

$$\mu_{\hat{H}} = \frac{1}{n}\sum_{u=1}^{n} \hat{H}(u) \quad \ldots\ldots (9)$$

The basic idea behind determining the length using an essential cross-correlation method is to obtain the actual blur width on the path based on the maximum cross-correlation. Obviously, the maximum cross correlation is in $g = [g(0)g(1)\ldots g(N-1)]^T$, which matches the logarithmic of the Fourier spectrum of the actual value of PSF $h$. In particular, the steps are as follows:

*i. According to blur angle $\theta$, choose blur center $(i, j)$ as the image center, and set the blur radius r (in this paper, $r = 50$).*

*ii. Extract the pixel grayscale on each blur direction using $(i, j)$ as the center. Use Eq. (7) to calculate the cross-correlation of candidate PSF $\hat{h}$.*

*iii. When blur radius r increases, blur width $\hat{a}_r$ on the blur path increases accordingly, and the ratio between r and $\hat{a}_r$ is expressed by a discrete line; the search stops, and the current $(i, j)$ is set as the actual blur center, with the current blur width as the actual blur width. Otherwise, perform step iv.*

*iv. Choose another blur center $(i, j)$ and repeat step ii until the conditions in step iii are satisfied.*

## 3. Description of Image Restoration Algorithm

Using the aforementioned method, the parameters of the noisy motion blur images, including motion blur angle and motion blur length, are estimated. When the motion blur parameters are determined, Eq. (4) is used to estimate PSF and set the number of iterations $N$ of the Lucy-Richardson algorithm [12] in order to restore the observed images blurred by movement. After a certain number of iterations, the blurred image is restored. The process for the image restoration algorithm is shown in **Fig. 4**.

## 4. Results and Analysis

The evaluation criteria [13] for restored images are various. In this paper, we use the objective evaluation criteria that includes Signal-to-Noise Ratio (SNR) and Peak Signal-to-noise ratio (PSNR):

$$SNR = 10 * \log_{10}\left[\frac{\sum_{i=1}^{M}\sum_{j=1}^{N} f(i,j)^2}{\sum_{i=1}^{M}\sum_{j=1}^{N}\left[f(i,j) - \hat{f}(i,j)\right]^2}\right] \quad (10)$$

$$PSNR = 10 * \log_{10}\left[\frac{255^2 \times M \times N}{\sum_{i=1}^{M}\sum_{j=1}^{N}\left[f(i,j) - \hat{f}(i,j)\right]^2}\right] \quad (11)$$

where $M$ and $N$ are the number of pixels on the image length and width, and $f(i, j)$ and $\hat{f}(i, j)$ are the gray value of the original image and the image being evaluated at point $(i, j)$.

To verify the effectiveness and reliability of our proposed algorithm, some recovery experiments on noisy motion blur images are performed on a PC (AMD Athlon (TM) II × 4,630, 2.0 G-memory) with MATLAB 7.0 simulation software algorithm programming.

### 4.1. Restoration Experiment on Artificial Blurred Images

For our experiment, we used the test images from [14]. We created a test bed that consists of standard images of size 256 × 256, such as Lena, Weixing, Camera man, etc., degraded by different motion blur parameters. Then we added additive Gaussian noise to these images.

In the experiment, we used the artificial blurred image Weixing. First, we added different level noises to the original image, as shown in **Fig. 5**. **Fig. 5(a)** is the original

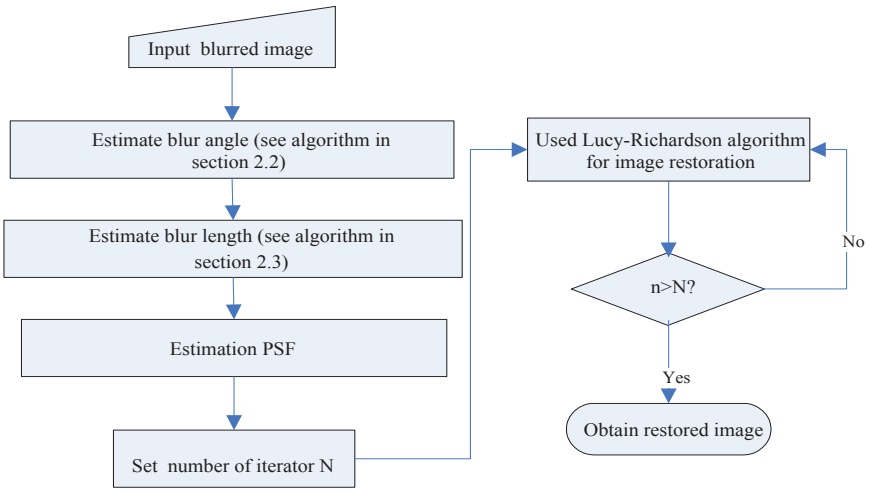


**Fig. 4.** Flowchart for image restoration algorithm.

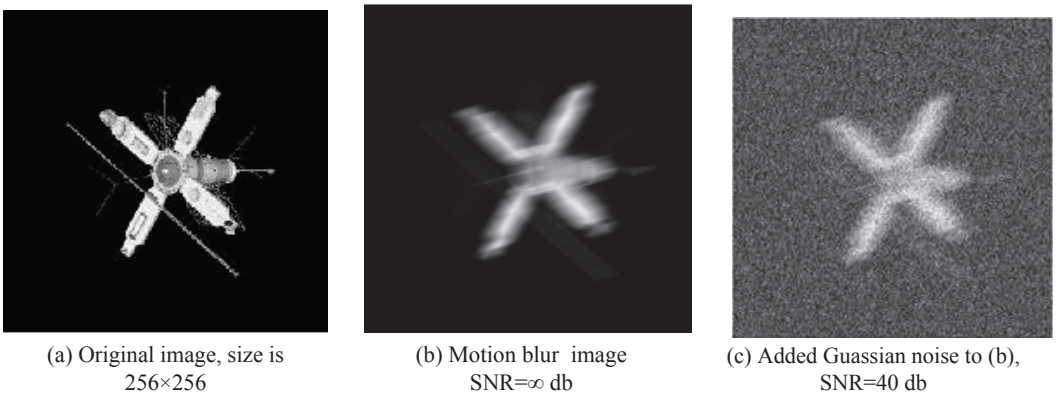

(a) Original image, size is 256×256

(b) Motion blur image SNR=∞ db

(c) Added Guassian noise to (b), SNR=40 db

(d) Added Guassian noise to (b), SNR=30 db

(e) Added Guassian noise to (b), SNR=20 db

**Fig. 5.** Motion blur images.

Weixing image of size $256 \times 256$. Its motion blurred image is shown in **Figs. 5(b)**, **5(c)**, **5(d)**, and **5(e)**. The actual motion blur angle is 15°; fuzzy length is 19 pixels; SNR = ∞ dB (noise-free). Then we added white Gaussian noise to **Fig. 5(b)** with SNRs of 40 dB, 30 dB, and 20 dB, as shown in **Figs. 5(c)**, **5(d)**, and **5(e)**.

We test the effectiveness of fuzzy length calculation using the cross-correlation method. According to the estimation algorithm described in Section 2.3, we estimate the blur angle of the image shown in **Fig. 6** using the algorithm described in Section 2.2 with exposure time movement angle of 15° and the center of the image as the blur center, then we select the blur path with a blur radius $r$ of 70 as an example. The blur length of the path should be as follows:

$$a = 1 + \left( \int \right) 70 \times \pi \times \frac{15^\circ}{180^\circ} = 19 \quad . \quad . \quad . \quad . \quad . \quad (12)$$

The cross-correlation data is obtained by Eq. (7), its maximum value is stable at $a = 19.2$. The motion blur image restoration results applied to the images shown in **Fig. 5** are shown in **Fig. 6**. This paper uses the Lucy-Richardson algorithm with 100 times iterations.

It can be seen from the restored images and PSNR re-

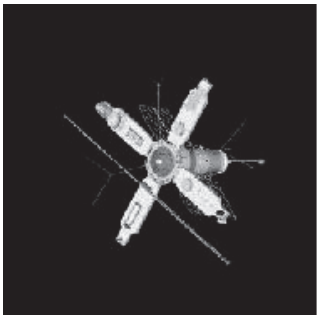

(a) Restored image from Fig.5 (b)

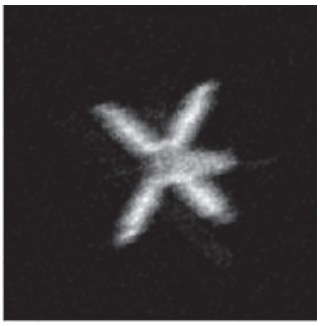

(b) Restored image from Fig.5 (c)

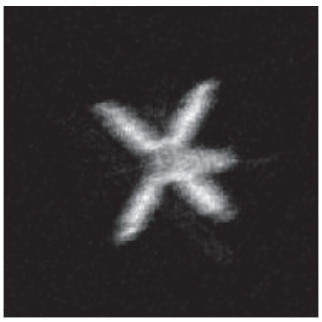

(c) Restored image from Fig.5 (d)

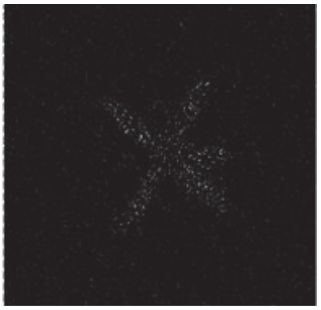

(d) Restored image from Fig.5 (e)

**Fig. 6.** Motion blur image restoration with different noise levels.

sults that when the noise has SNR = 30 dB, recovery using our proposed algorithm occurs relatively well. When SNR = 20 dB, the effect of the recovery is bad. Various PSNR values under different SNR are listed in **Table 1**.

We can see that, when SNR = 40 dB, the PSNR value is 30.39; when SNR = 30 dB, the PSNR value is 27.46; finally, when the blurred image's SNR = 20 dB, its PSNR value is only 16.59. Our algorithm for motion blur image (blur + noise) demonstrates good recovery effect. Naturally, in the case of a limited number of iterations, the observed image is completely recovered when the iteration times increase, but the time required for the process also increases.

**Table 1.** PSNR values under different SNRs.

| Image | Fig. 6(a) | Fig. 6(b) | Fig. 6(c) | Fig. 6(d) |
|---|---|---|---|---|
| **SNR (dB)** | ∞ | 40 | 30 | 20 |
| PSNR(dB) | 40.73 | 30.39 | 27.46 | 16.59 |

(a) Taj Mahal motion blur image

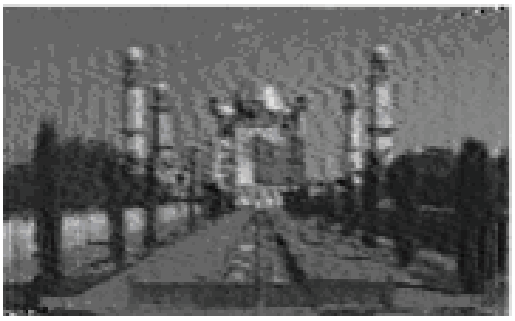

(b) Restored image by Wiener filtering algorithm

(c) Restored image by our algorithm

**Fig. 7.** Restoration results of Taj Mahal motion blur image.

### 4.2. Restoration Experiment on Naturally Blurred Church Images

We use the previous algorithm to manage temple images captured in a natural background; the processing results for a sample image (the Taj Mahal mosque) are shown in **Fig. 7**. **Fig. 7(a)** is a naturally blur image, **Fig. 7(b)** is the image restored by the Wiener filtering algorithm, and **Fig. 7(c)** is image restored by our algorithm. By comparing the noisy motion blur situation of **Figs. 7(b)** and **7(c)**, we can see that the restoration results of the Wiener filtering algorithm make the image edges

**Table 2.** Restoration time comparison of two algorithms.

| Algorithm | Restoration time(s) |
|---|---|
| Wiener filtering algorithm | 1.172 354 |
| Our algorithm | 0.845 822 |

very fuzzy, whereas the restoration effect of our algorithm has a much clearer edge and strong noise resistance.

**Table 2** lists the comparison results of the time required by the two methods used for the image restoration of this experiment. Through the experiment, we can see that the image restoration algorithm proposed in this paper can make image restoration better; meanwhile, the algorithm has a greatly reduced restoration time. This proves that our algorithm has the characteristics of rapidity. This algorithm is processed in the frequency domain, which can greatly save CPU costs. Compared with the other deconvolution algorithm, ours can increase the efficiency of image restoration, and it is suitable for real-time engineering requirements.

## 5. Conclusion

This paper proposed a motion blur angle estimation method based on the Radon transform, blur parameter identification, and cross-correlation computing blur length estimation method based on the movement of cross-correlation. These methods were applied not only to the uniform identification of blur parameters, but also to variable-speed linear motion of the acceleration. The restoration exercise had a strong anti-noise ability to identify high precision for blur image. The theoretical and experiment results described in this paper showed that our algorithm can execute good recovery for both artificially and naturally (camera shake) blurred images.

**Acknowledgements**

This research is supported by the Scientific and Technological Research Project of Jilin Province Department of Education (No. 2013145, No. 201363).

**References:**

[1] M. Ben-Ezra and Nayar, "Motion deblurring using hybrid imaging," IEEE Conf. on Computer Vision and Pattern Recognition, Madison, Winsconsin, pp. 454-460, 2003.

[2] T. F. Chan and C. K. Wong, "Total variation blind deconvolution," IEEE Trans. Image Process, Vol.7, No.3, pp. 370-375, 1998.

[3] C. Mayntz and T. Aach, "Blur identification using a spectral inertia tensor and spectral zeros," Proc. IEEE Int. Conf. Image Proc, pp. 885-889, 1999.

[4] M. M. Chang, A. M. Tekalp, and A. T. Erdem, "Blur identification using the bispectrum," IEEE Trans. Acoust. Speech Signal Process, Vol.39, pp. 2323-2325, 1991.

[5] Z. Yu and Z. Xu-sheng, "An improved motion blur image restoration algorithm," Computer Engineering and Science, Vol.31, No.10, pp. 491-500, 2009.

[6] M. R. Baham and A. K. Katsagellos, "Digital image restoration," IEEE Signal Processing Magazine, Vol.14, No.2, pp. 24-41, 1997.

[7] M. Ebranhimi Moghaddam and M. Jamzad, "Motion blur identification in noisy images using mathematical models and statistical measures," Pattern Recognition, Vol.40, pp. 1946-1957, 2007.

[8] H. Haogang and L. Yan-ling, "Blurred Image Restoration based on the movement of direction information measure," Computer Engineering, Vol.36, No.2, pp. 201-202, 2010.

[9] Z. De, "Digital Image Processing (MATLAB)," Beijing: Posts & Telecom Press, pp. 176-184, 2009.

[10] G. Bonmassar and E. L. Schwartz, "Real-time restoration of images degraded by uniform motion blur in foveal active systems," IEEE Trans. on Image Processing, Vol.8, No.12, pp. 1838-1842, 1999.

[11] H. Hanyu and Z. Tianxu, "Fast restoration approach for rotational motion blurred image based on deconvolution along the blurring paths," Optical Engineering, Vol.42, No.12, pp. 3471-3486, 2003.

[12] Y. Yitzhaky, I. Mor, and A. Lantzman, "A direct method for restoration of motion blurred images," J. Opt. Soc. Am. A, Vol.15, No.6, pp. 1512-1519, 1998.

[13] M. R. Banham and A. K. Katsagellos, "Digital image restoration," IEEE Signal Processing Mag., 14, pp. 24-41, 1997.

[14] USC-SIPI Image Database, Online Image Database Available: http://sipi.usc.edu/database [Accessed May 2015]

**Name:**
Li Dongming

**Affiliation:**
Professor, Department Head, School of Information Technology, Jilin Agriculture University

**Address:**
No.2888, XinCheng Street, Changchun City, Jilin Province, China

**Brief Biographical History:**

2001 Received Bachelor degree from Jilin Normal University
2001-2006 Teaching Assistant, School of Information Technology, Jilin Agriculture University
2007-2011 Lecturer, School of Information Technology ,Jilin Agriculture University
2009 Received Master degree from Changchun University of Technology
2012- Associate Professor, School of Information Technology, Jilin Agriculture University

**Main Works:**

• L. Dongming, S. Wei, et al., "Target Image Matching Algorithm Based on Binocular CCD Ranging," Abstract and Applied Analysis, Vol.2014, DOI:10.1155/2014/785072, July 2014.
• L. Dongming, G. Mengye, et al., "Research on Adaptive Optics Image Denoising Algorithm Based on the Wavelet-Based Contourlet Transform," Laser & Optoelectronics Progress, Vol.52, 111001-1-10, Nov. 2015.
• L. Dongming, et al., "Research on Wavefront Correction Algorithm of Adaptive Optics System," ICCSNT2015, pp. 2219-2226, Dec. 2015.
• L. Dongming, Z. Lijuan, et al., "Chinese Learning of Semantical Selectional Preferences Based on LSC Model and Expectation Maximization," J. of Software, Vol.7, 2488-2493, Nov. 2012.

**Membership in Academic Societies:**

• The Standing Director of Jilin Youth Workers Association

**Name:**
Su Zhengbo

**Affiliation:**
School of Computer Science and Technology, Harbin Institute of Technology

**Address:**
92 West Dazhi Street, Harbin, Heilongjiang Province, China

**Brief Biographical History:**

2012- Enrolled in Harbin Institute of Technology

**Name:**
Su Wei

**Affiliation:**
Professor, Informatization Center, Changchun University of Science and Technology

**Address:**
No.7089, Rd. Weixing, Changchun, Jilin Province, China

**Brief Biographical History:**
1990- Joined Changchun University of Science and Technology
2006-2007 Visiting Researcher, Tokyo Institute of Technology

**Main Works:**
• Z. Lijuan, L. Dongming, S. Wei, et al., "Research on Adaptive Optics Image Restoration Algorithm by Improved Expectation Maximization Method," Abstract and Applied Analysis, Vol.2014, p. 10, DOI:10.1155/2014/781607, July 2014.
• L. Dongming, S. Wei, et al., "Target Image Matching Algorithm Based on Binocular CCD Ranging," Abstract and Applied Analysis, Vol.2014, DOI:10.1155/2014/785072, July. 2014.
• L. Dongming, S. Wei, and Z. Lijuan, "Based on B-splines Non-rigid Registration Method of Atmospheric Turbulence Image," ASPIRE 2012, Nov. 2012.
• Z. Lijuan, Y. Jinhua, and S. Wei, "Multi-frame Iteration Blind Deconvolution Algorithm Based on Improved Expectation Maximization for Adaptive Optics Image Restoration," Acta Armamentarii, Vol.31, pp. 1765-1773, Nov. 2014.

**Membership in Academic Societies:**
• Member of China Higher Education Information Academy
• Vice President of Jilin Province Education Informatization Association of China

**Name:**
Zhang Lijuan

**Affiliation:**
Associate Professor, College of Computer Science and Engineering, Changchun University of Technology

**Address:**
No.2055, YanAn Street, Changchun City, Jilin Province, China

**Brief Biographical History:**
2001 Received Bachelor degree from Jilin Normal University
2004 Received Master degree from Changchun University of Science and Technology
2004-2006 Teaching Assistant, College of Computer Science and Engineering, Changchun University of Technology
2007-2012 Lecturer, College of Computer Science and Engineering, Changchun University of Technology
2013- Associate Professor, College of Computer Science and Engineering, Changchun University of Technology
2015 Received Doctor degree from Changchun University of Science and Technology

**Main Works:**
• Z. Lijuan, L. Dongming, S. Wei, et al., "Research on Adaptive Optics Image Restoration Algorithm by Improved Expectation Maximization Method," Abstract and Applied Analysis, Vol.2014, p. 10, DOI:10.1155/2014/781607, July. 2014.
• Z. Lijuan, Y. Jinhua, et al., "Research on Blind Deconvolution Algorithm of Multi-Frame Turbulence Degraded images," J. of Information and Computational Science, Vol.10, pp. 3625-3634, Oct. 2013.
• Z. Lijuan, Y. Jinhua, and S. Wei, "Multi-frame Iteration Blind Deconvolution Algorithm Based on Improved Expectation Maximization for Adaptive Optics Image Restoration," Acta Armamentarii, Vol.31, pp. 1765-1773, Nov. 2014.
• Z. Lijuan and L. Dongming, "High-accuracy image registration algorithm using B-splines," ICCSNT2012, pp. 279-283, Dec. 2012.

**Membership in Academic Societies:**
• The Standing Director of Jilin Youth Workers Association